

# Supporting Information for Magnesium Ion Mobility in Post-Spinels Accessible at Ambient Pressure

Daniel C. Hannah,<sup>†</sup> Gopalakrishnan Sai Gautam,<sup>‡,†,¶</sup> Pieremanuele Canepa,<sup>†,‡</sup>  
Ziqin Rong,<sup>‡</sup> and Gerbrand Ceder\*,<sup>¶,†,‡</sup>

<sup>†</sup> *Materials Science Division, Lawrence Berkeley National Laboratory, Berkeley, CA 94720,  
USA*

<sup>‡</sup> *Department of Materials Science and Engineering, Massachusetts Institute of Technology,  
Cambridge, MA 02139, USA*

<sup>¶</sup> *Department of Materials Science and Engineering, University of California Berkeley, CA  
94720, USA*

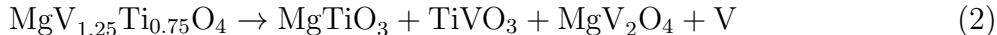
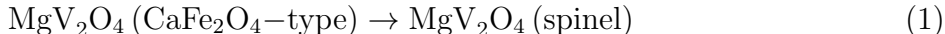
E-mail: gceder@berkeley.edu, gceder@lbl.gov

# 1 Computational Methodology

We utilize density functional theory (DFT)<sup>1</sup> as implemented in the Vienna *ab initio* Simulation Package (VASP).<sup>2,3</sup> The exchange-correlation functional were approximated by the Perdew-Burke-Ernzerhoff (PBE) implementation of the Generalized Gradient Approximation (GGA) functional.<sup>4</sup> The wavefunctions were described by the Projector Augmented Wave (PAW)<sup>5</sup> theory combined with a kinetic energy cutoff of 520 eV and were sampled on a Monkhorst-Pack mesh with a  $k$ -point density of 1000/(number of atoms in the unit cell). For voltage and stability calculations, spurious self-interaction errors on  $d$ -electrons were accounted for by adding a Hubbard- $U$  correction.<sup>6,7</sup> The  $U$  values obtained by Jain *et al.* were used.<sup>8</sup> Ionic migration barriers were calculated using the Nudged Elastic Band (NEB) method<sup>9</sup> with a total of 9 images between the endpoints. Standard GGA is used in the NEB calculations owing to the problematic convergence of GGA+ $U$  NEB calculations.<sup>10</sup>

## 2 Decomposition reactions for magnesiated V/Ti post-spinel compounds

Based on phase diagrams constructed using the Materials Project database,<sup>11</sup> we display below the predicted decomposition reactions for the metastable  $\text{MgV}_{2-x}\text{Ti}_x\text{O}_4$  ( $x = 0, 0.75, 2$ ) materials:



### 3 Voltage curves for V/Ti post-spinel compounds

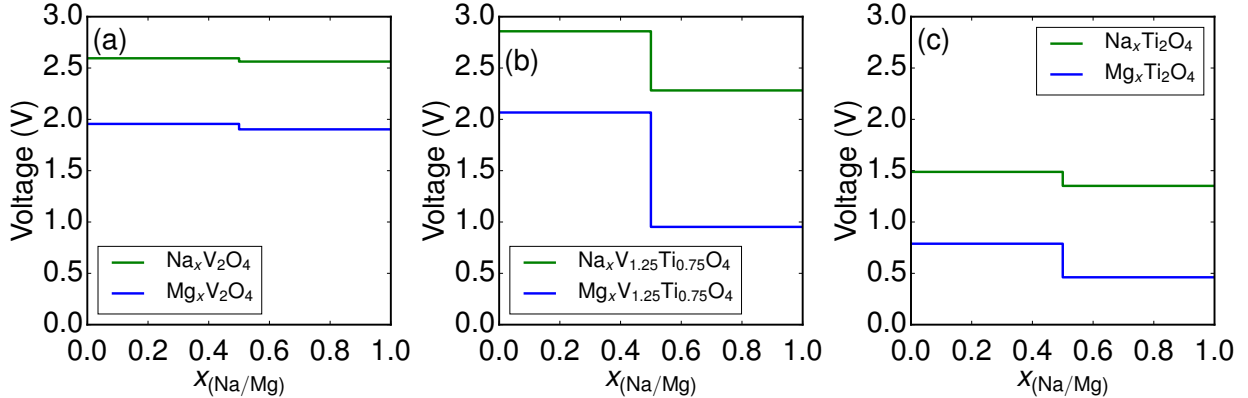


Figure 1: Voltage as a function of the extent of sodiation/magnesium for (a)  $\text{V}_2\text{O}_4$ , (b)  $\text{V}_{1.25}\text{Ti}_{0.75}\text{O}_4$ , (c)  $\text{Ti}_2\text{O}_4$ . The structures at  $x = 0.5$  were taken to be the lowest energy structures among possible working ion/vacancy orderings at this concentration.

Figure 1 displays the voltages for V and Ti-containing post-spinel compounds at 0, 50, and 100% sodiation (magnesium). The structures at 50% discharge ( $x = 0.5$ ) were taken to be the lowest-energy structures among all possible working ion/vacancy orderings in a  $3 \times 1 \times 1$  supercell with 50% A-site occupancy. As with the voltage data presented in the main manuscript, voltages were calculated using the free energy change of the intercalation reaction to a particular concentration (i.e. 50 or 100 %).

### 4 Comparison of stable sites and migration paths for Na and Mg ions

The stable sites for Na and Mg differ in displacement from the channel centroid, which is indicated by a dashed circle in in Figures 2a and 2c. The stable site for Na (Fig. 2a) is in a part of the channel which is 17.5% larger in the  $b$  direction compared to the stable site for Mg (Fig. 2c). The absolute distances between channel walls in the  $b$  direction are indicated by black double-sided arrows on Figs. 2a and 2c. The differences in stable site result in a

slightly different migration path for Na and Mg. The paths are compared in Figures 2b and 2d. The Mg ion first moves along the  $c$  direction into a more central part of the channel before migrating along a roughly linear trajectory followed by a move back to the stable Mg site. During movement along the  $c$  axis the Mg ion passes through a distorted square plane of oxygen atoms, creating a local activated state which manifests as the multi-peaked energy profile for migration (Fig. 3b, d, f in the main manuscript). In contrast, the motion of the Na ion is predominantly in the  $a$  direction and only a single maximum is observed (Fig. 3a, c, e in the main manuscript). In the discharged limit, the Mg site more closely resembles the Na site, resulting in a migration energy profile similar to the one observed for Na ions (Fig. 3 in the main manuscript).

## References

- (1) Kohn, W.; Sham, L. J. Self-consistent equations including exchange and correlation effects. *Physical Review* **1965**, *140*, A1133.
- (2) Kresse, G.; Hafner, J. Ab initio molecular dynamics for liquid metals. *Physical Review B* **1993**, *47*, 558.
- (3) Kresse, G.; Furthmüller, J. Efficient iterative schemes for ab initio total-energy calculations using a plane-wave basis set. *Physical Review B* **1996**, *54*, 11169.
- (4) Perdew, J. P.; Burke, K.; Ernzerhof, M. Generalized gradient approximation made simple. *Physical Review Letters* **1996**, *77*, 3865.
- (5) Kresse, G.; Joubert, D. From ultrasoft pseudopotentials to the projector augmented-wave method. *Physical Review B* **1999**, *59*, 1758.
- (6) Anisimov, V. I.; Zaanen, J.; Andersen, O. K. Band theory and Mott insulators: Hubbard U instead of Stoner I. *Physical Review B* **1991**, *44*, 943.
- (7) Zhou, F.; Cococcioni, M.; Marianetti, C. A.; Morgan, D.; Ceder, G. First-principles prediction of redox potentials in transition-metal compounds with LDA+ U. *Physical Review B* **2004**, *70*, 235121.
- (8) Jain, A.; Hautier, G.; Ong, S. P.; Moore, C. J.; Fischer, C. C.; Persson, K. A.; Ceder, G. Formation enthalpies by mixing GGA and GGA+ U calculations. *Physical Review B* **2011**, *84*, 045115.
- (9) Sheppard, D.; Terrell, R.; Henkelman, G. Optimization methods for finding minimum energy paths. *The Journal of Chemical Physics* **2008**, *128*, 134106.

- (10) Liu, M.; Rong, Z.; Malik, R.; Canepa, P.; Jain, A.; Ceder, G.; Persson, K. A. Spinel compounds as multivalent battery cathodes: a systematic evaluation based on ab initio calculations. *Energy & Environmental Science* **2015**, *8*, 964–974.
- (11) Jain, A.; Ong, S. P.; Hautier, G.; Chen, W.; Richards, W. D.; Dacek, S.; Cholia, S.; Gunter, D.; Skinner, D.; Ceder, G.; ; Persson, K. Commentary: The Materials Project: A materials genome approach to accelerating materials innovation. *Appl Materials* **2013**, *1*, 011002.

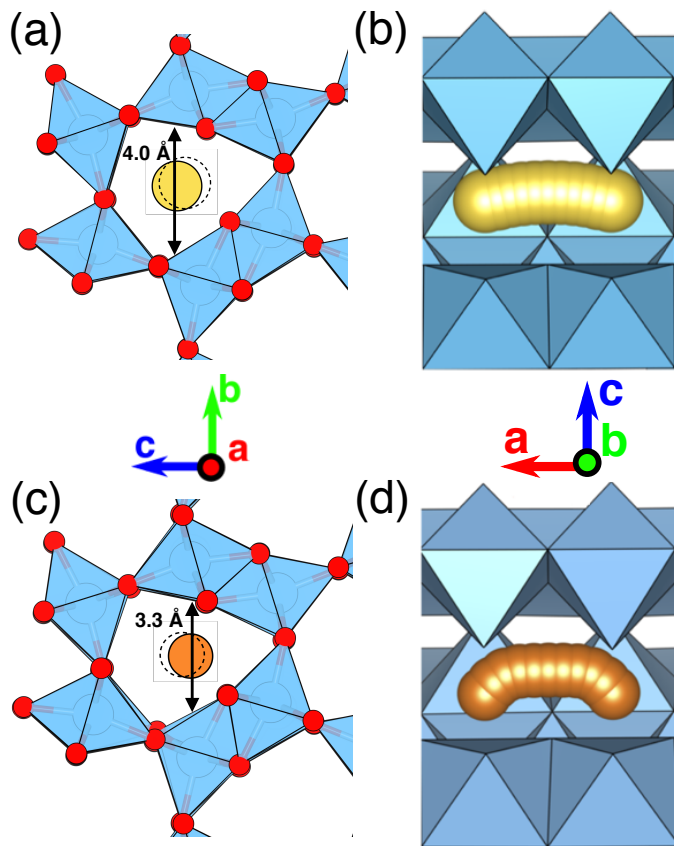


Figure 2: (a) Na ion position obtained following DFT relaxation of the charged state structure of Na in  $\text{Ti}_2\text{O}_4$ . The concentric circle represents the channel "center" defined here as the geometric centroid of the 8 coordinating oxygen atoms. The black arrow and label indicate the distance between channel walls in the  $b$  direction. (b) Minimum energy migration path for Na in  $\text{Ti}_2\text{O}_4$  derived from NEB calculations in the charged limit. (c) Mg ion position obtained following DFT relaxation of the charged state structure of Mg in  $\text{Ti}_2\text{O}_4$ . The labels on the figure have the same meaning as in (a). (d) Minimum energy migration path for Mg in  $\text{Ti}_2\text{O}_4$  derived from NEB calculations in the charged limit. The compass on the left applies to (a) and (c), while the compass on the right applies to (b) and (d).